Available online at www.sciencedirect.com

ScienceDirect

Journal of the European Ceramic Society 29 (2009) 3293–3297

www.elsevier.com/locate/jeurceramsoc

Technical note

Improvement of the high temperature properties of the $LiYO_2$–Si_3N_4 system by removing residual Li

Sea-Hoon Lee [a,*], Reinhard Mager [b]

[a] *Korea Institute of Materials Science (KIMS), 531 Changwondaero, Changwon, Gyeongnam 641-831, Republic of Korea*
[b] *Max-Planck-Institut für Metallforschung and Institut für Nichtmetallische Anorganische Materialien, Pulvermetallurgisches Laboratorium, Heisenbergstrasse 3, 70569 Stuttgart, Germany*

Received 13 February 2009; received in revised form 24 May 2009; accepted 11 June 2009

Abstract

Effects of the vaporization of residual Li on the microstructure, oxidation behavior and high temperature properties of a low-temperature pressureless sintered Si_3N_4 using $LiYO_2$ additive were investigated. The oxidation and creep resistance of the Si_3N_4 was improved after an annealing at 1650 °C because residual Li, which deteriorated the high temperature properties of the Si_3N_4, could be mostly removed. The high temperature deformation of the Si_3N_4 was strongly suppressed after the annealing treatment. The annealed specimens retained 64% of the room temperature strength at 1300 °C in air. The present investigation reports a method to improve the high temperature properties of Si_3N_4.

Keywords: Impurities; Creep; Thermal properties; Si_3N_4; Annealing

1. Introduction

Si_3N_4 has excellent mechanical and high temperature properties. However, its industrial application has been limited so far partly due to the high production cost. Accordingly, low-temperature pressureless sintering of Si_3N_4 has received strong interest recently.[1]

Several additives have been applied for the pressureless sintering of Si_3N_4.[2,3] Among them, $LiYO_2$ has been considered as a challenging candidate.[4,5] The present authors fabricated Si_3N_4 specimens having high strength (600–700 MPa) and moderate fracture toughness (5–6 $MPa\sqrt{m}$) by pressureless sintering at 1600 °C.[6]

Several methods have been reported in order to improve the high temperature properties of Si_3N_4. Additives having high eutectic temperature with SiO_2, such as rare-earth oxides, have successfully improved the high temperature properties of Si_3N_4.[7] However, high temperature and pressure were generally required for the densification because of the high refractoriness of the additives. Crystallization of amorphous grain boundary phases within Si_3N_4 has been reported as an alternative method.[8] In this case low-temperature sintering of Si_3N_4 was possible, but often annealing treatments for the crystallization required prolonged processing time above several hundreds of hours.[8] In addition, the strength of the crystallized specimens was often inferior to that of the as-sintered ones.[8]

Li_2O, which strongly decreases the softening temperature of the grain boundary phase in Si_3N_4 (eutectic temperature of $LiYO_2$ with SiO_2: 1255 °C), vaporizes rapidly above 1550 °C.[4,9] The reduction of residual Li content in the $LiYO_2$–Si_3N_4 system after annealing treatments has been reported.[4,6] However, the effects of annealing treatments on the improvement of high temperature properties such as oxidation resistance, creep resistance and high temperature strength have never been investigated. Here we report the improvement of the high temperature properties of the $LiYO_2$–Si_3N_4 system by removing Li through annealing treatments.

2. Experimental procedure

Si_3N_4 (SN-E10, UBE), Y_2O_3 (Grade C, H.C. Starck) and Li_2CO_3 (Chemical Lab.) were used as starting materials. Y_2O_3 and Li_2CO_3 were mixed (1:2.04 by mole%) and calcined at 1400 °C for 4 h in air to synthesize $LiYO_2$.[4] The mixture

---

* Corresponding author. Tel.: +82 55 280 3344; fax: +82 55 280 3392.
E-mail address: seahoon1@kims.re.kr (S.-H. Lee).

0955-2219/$ – see front matter © 2009 Elsevier Ltd. All rights reserved.
doi:10.1016/j.jeurceramsoc.2009.06.021

Table 1
Residual Li content of the specimens before and after annealing treatment, and flexural strength of the 1650-specimens at 25 or 1300 °C in air. Li content was measured at the central area of large sintered blocks.

$LiYO_2$ content (wt%)	Li content (wt%)			Strength (MPa)	
	As-sintered	As-annealed		25 °C	1300 °C
		1600 °C	1650 °C		
7.5	0.41	0.24	0.008	674 ± 101	431 ± 90
10	0.52	0.33	0.022	598 ± 85	286 ± 43
12.5	0.68	0.4	0.061	584 ± 106	246

of Si_3N_4 and 7.5, 10, 12.5 wt% $LiYO_2$ powder (termed 7.5-, 10- and 12.5-specimen, respectively) was compacted by a cold isostatic press (CIP, pressing condition: 240 MPa, 3 min) and the compacts were pressureless sintered at 1600 °C for 2 h in 0.1 MPa N_2 (termed as-sintered specimen, heating rate: 10 °C/min). Then, the specimens were annealed sequentially at 1550 and 1600 °C (termed 1600-specimen) or 1550 and 1650 °C (termed 1650-specimen) for 8 h in 0.1 MPa N_2. The residual Li content, microstructure and phase composition of the as-sintered or annealed specimens was measured by inductively coupled plasma-optical emission spectrometry (ICP-OES, CIROS^{CCD}, Spectro), scanning electron microscopy (SEM, 4000, Jeol) and X-ray diffraction with Cu Kα_1 radiation, equipped with a quartz primary monochromator (XRD, D5000, Siemens).

In order to measure oxidation behavior, the annealed specimens were polished up to 1 μm finish and were cleaned sequentially by de-ionised water, isoprophyl alcohol and acetone. The weight gain during oxidation was analyzed up to 1400 °C (3 °C/min) using a thermo-gravimetric analyzer (TGA, STA 409C, Netzsch) in flowing air (100 ml/min).

The 1650-specimens were machined into bend bars (50 mm × 3 mm × 4 mm) and were polished down to 1 μm finish for 4-point bending test at room temperature and at 1300 °C in air (1476, Zwick, crosshead speed: 100 μm/min, upper and lower span: 10 and 40 mm).[10] At least five specimens were used for the room temperature bending test except for the 12.5-1650 system (three specimens). The 7.5- and 10-1650 specimens were tested four and three times at 1300 °C, while testing of the 12.5-1650 specimen was stopped after the first measurement in order to prevent the damage of the equipment due to the softening and strong deformation of the sample. During the high temperature testing, a 7.5-1650 specimen was broken at a very low stress due to large surface flaws. Because the result did not reflect the effect of residual Li on the high temperature strength, the data was not used for analysis. Young's modulus, hardness and fracture toughness of the samples were measured using an ultrasonic tester (5072PR, Panametrics) and Vickers indenter (AVK-A, Akashi, loading condition: 10 kg, 15 s). The measurements were performed at least five times per each condition. Fracture toughness was calculated using the formula proposed by Anstis et al.[11]

The surface of the specimens tested at 1300 °C in air was analyzed by SEM and X-ray powder diffraction (XRD, JDX-3500, JEOL) with Cu Kα radiation.

3. Results and discussion

Table 1 shows the residual Li content within the specimens before and after annealing treatment. The theoretical Li content of the 7.5, 10 and 12.5 wt% $LiYO_2$–Si_3N_4 system was 0.41, 0.54 and 0.68 wt%, respectively. The Li content of the as-sintered specimens (0.41, 0.52, 0.68 wt%, respectively) was almost identical with the theoretical values, indicating that the vaporization of Li_2O did not occur inside the specimens during sintering.[6] The amount of residual Li decreased by annealing treatment at 1600 °C and the behavior became distinct at 1650 °C.[12] As a result, residual Li content was reduced down to 0.008 wt% (7.5-1650 specimen, Table 1). The value increased with the amount of the additive.[6]

In spite of the decrease of Li content by vaporization after the annealing of the 7.5-specimens, their apparent density increased by the treatment (7.5-as-sintered and 7.5-1650 specimen: 3.05 and 3.16 g/cm^3). Fig. 1 shows the reduction of the number and size of the pores in the 7.5-as-sintered specimen after the annealing at 1650 °C, indicating that the formation of pores by the vaporization of Li_2O during the annealing was compensated by densification. Fine grains ($\leq$0.3 μm) in the 7.5-as-sintered specimen were essentially eliminated in the 7.5-1650 specimen because of grain growth. Growth of large grains at the expense of smaller ones (Ostwald ripening) occurred during the annealing treatment.[13] XRD analysis indicated that the phase transformation from α- to β-Si_3N_4 was completed in the 7.5-as-sintered specimen (data not shown). The reflections of Y-apatite ($Y_5Si_3O_{12}N$) were reduced after annealing the 7.5-as-sintered specimen at and above 1600 °C because the secondary phase was mostly dissolved into a liquid phase during the annealing.[14]

The strength, Young's modulus and hardness of the 7.5-as-sintered specimen (630 ± 115 MPa, 258 ± 3 GPa and 11.6 ± 0.1 GPa, respectively) were only slightly improved (5–15%) after the annealing at 1650 °C (674 ± 101 MPa, 271 ± 8 GPa and 13.3 ± 0.3 GPa). The improvement of mechanical properties by the annealing was attributed to the densification of the rather porous as-sintered specimen. Fracture toughness of the 7.5-as-sintered specimen did not change greatly after the annealing at 1650 °C (5.5 ± 0.3 MPa m$^{1/2}$ *vs.* 5.3 ± 0.2 MPa m$^{1/2}$). The 7.5-specimens showed crack deflection behavior regardless of the annealing treatment (Fig. 1).

Fig. 2 shows the weight gain of the annealed specimens during TGA measurement in air. The mass of the 1600-specimens began to increase above 800 °C because of oxidation, and the weight gain became intensive above 1200 °C. $LiYO_2$ strongly decreases the melting temperature of SiO_2.[4] The fast oxidation of the 1600-specimens was most probably due to the low viscosity of the protective silicate layer formed by oxidation. The migration of oxygen through the protective silicate layer on Si_3N_4 was reported to be enhanced as the viscosity of the layer decreased.[15] In addition, bubbles were formed by the vaporization of Li_2O and/or by the following reactions, which also decreases the protective effect of the silicate layer[16];

$$2Si_3N_{4(s)} + 3O_{2(g)} \rightarrow 6SiO_{(g)} + 4N_{2(g)}, \tag{1}$$

$$Si_3N_{4(s)} + 3O_{2(g)} \rightarrow 3SiO_{2(s)} + 2N_{2(g)}. \tag{2}$$

In contrast to the 1600-specimen, weight gain by oxidation did not strongly occur in the 1650-specimen regardless of the additive content. The distinct improvement of oxidation resistance was unequivocally due to the strong reduction of residual Li content by the annealing treatment at 1650 °C. Chen et al. reported that the weight gain of Y_2O_3–Si_3N_4 system by oxidation did not strongly occur at 1350 °C, but became distinct at 1450 °C.[17] A similar result was reported by Govila et al.[18]

The creep resistance and high temperature strength of the specimens were clearly improved by reducing residual Li content. The onset stress of non-linear deformation at 1300 °C in air decreased with increasing the amount of additive and residual Li content (Fig. 3). Y_2O_3 and SiO_2 have a high eutectic temperature (1660 °C),[19] thus Si_3N_4 sintered with Y_2O_3 additive was reported to have high creep resistance.[20] However, the onset stress of deformation of the 10-1650 specimen was below 100 MPa, and strong deformation occurred before fracture (Fig. 3). On the other hand, the 7.5-1650 specimen showed brittle fracture behavior at 1300 °C. The residual Li content was believed to be the main reason for the difference between the annealed 7.5- and 10-1650 specimen. The 12.5-1650 specimen showed large deformation before fracture (data not shown). The results indicated that even rather small amount of residual Li (0.022–0.061 wt%) deteriorated the creep of Si_3N_4 at 1300 °C and also indicated that high temperature deformation of this system could be largely suppressed when residual Li was reduced to below 0.01%.

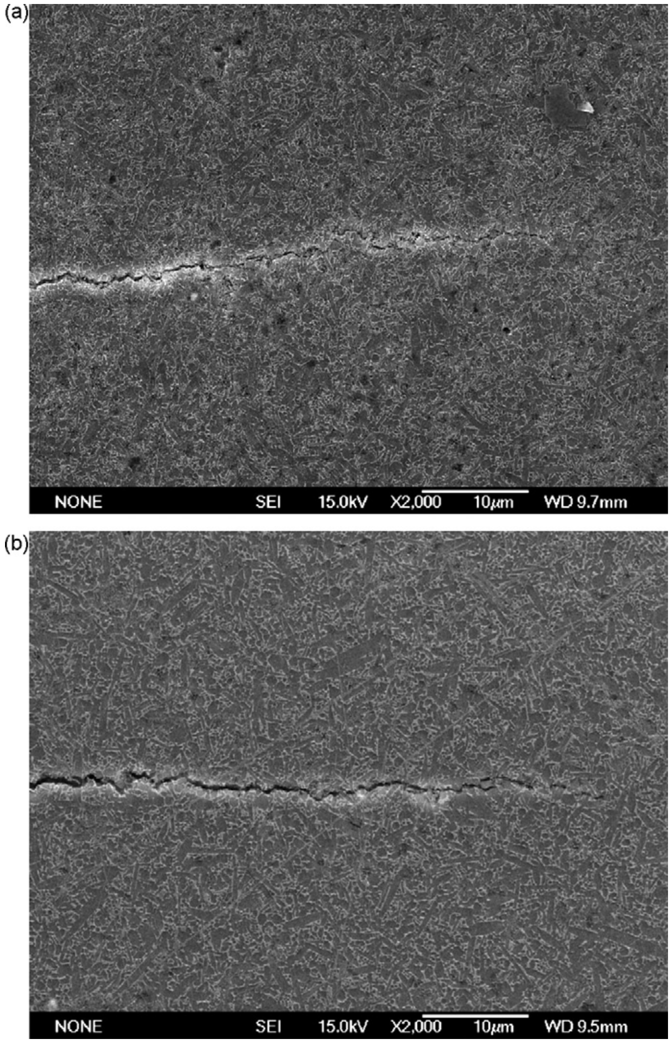

Fig. 1. Microstructure of (a) 7.5-as-sintered and (b) 7.5-1650 sample after indentation test (2000×).

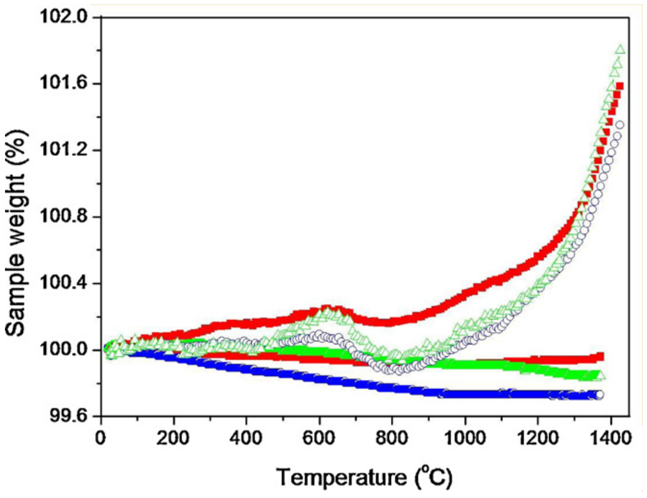

Fig. 2. Weight gain by oxidation during TGA measurement in air with the variation of additive contents and annealing conditions. Upper data: 1600-specimens, lower data: 1650-specimens ($LiYO_2$ content—■ : 7.5 wt%, □ : 10 wt% and ○ : 12.5 wt%).

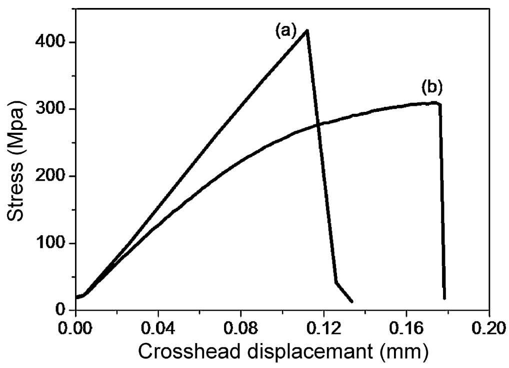

Fig. 3. Stress–displacement plots of specimens at 1300 °C in air. (a) 7.5-1650 and (b) 10-1650. Data of the 12.5-1650 specimen was not shown because of the strong creep deformation before fracture.

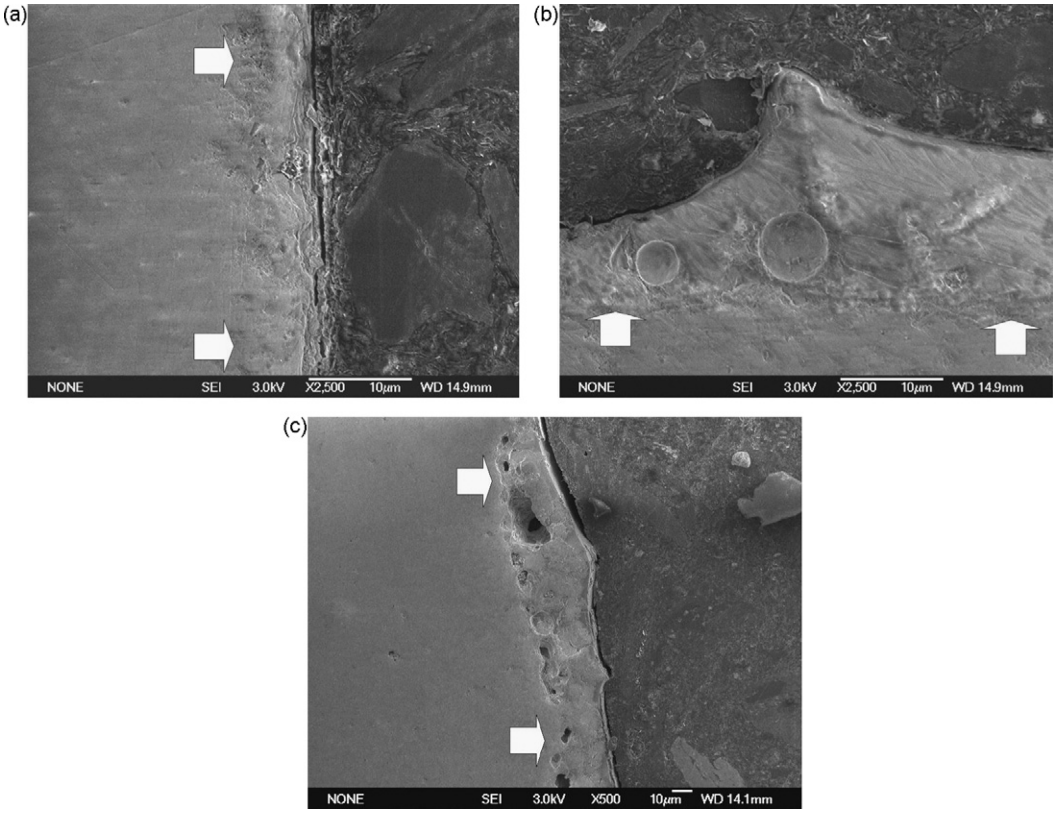

Fig. 4. Polished cross-section of sample surface after the high temperature bending test. (a) and (b) 7.5-1650 (2500×) and (c) 12.5-1650 (500×) (⇨ : boundary between the oxide layer and Si_3N_4).

In spite of the substantial reduction of residual Li content by the annealing treatment, high temperature strength of the 10- and 12.5-1650 specimens decreased to 48 and 42% of the room temperature value, respectively (Table 1). In contrast, the 7.5-1650 specimens retained 64% of the room temperature strength at 1300 °C in air.

Fig. 4 shows the surface of the 1650-specimen after the bending test at 1300 °C in air. The formation of silicate layers was observed, the thickness of which increased with the additive content (7.5-1650 specimen: 5–7 μm, 10-1650 specimen: 10–13 μm, 12.5-1650 specimen: 20–25 μm). The oxidation resistance of the Y_2O_3–Si_3N_4 system has been reported to be superior to that of most of the other Si_3N_4 sintered with additives.[21] Chen et al. reported that after oxidation at 1450 °C for 100 h, the thickness of silicate layer formed on the surface of the Y_2O_3–Si_3N_4 system was less than 5 μm.[17] The thickness of the silicate layer observed in the present research was larger than the reported values of the Y_2O_3–Si_3N_4 system because of the residual Li. The result indicated that even very small amount of residual Li (0.008 wt%) promoted the oxidation of Si_3N_4. The bubbles in the silicate layer of the 7.5-1650 specimens were formed only in locally protruded areas (Fig. 4(b)) presumably due to the inhomogeneous distribution of Li_2O in the silicate layer and consequent local melting at 1300 °C (eutectic temperature of SiO_2–$LiYO_2$ and SiO_2–Y_2O_3: 1255 and 1660 °C, respectively).[4,19] On the other hand, intensive bubble formation occurred beneath the thick silicate layer in the 12.5-1650 specimen after the bending test (Fig. 4(c)) because of the detrimental effect of residual Li on the oxidation resistance of Si_3N_4. The intensive bubble formation was also observed in a Si_3N_4 containing Na ion at the surface.[22]

SiO_2 (cristobalite) and $Si_2Y_2O_7$ were formed within the silicate layer, the amount of which increased with the additive content (Fig. 5). During oxidation, additives within Si_3N_4 have been reported to migrate into the amorphous oxide layer, and silicate phases were crystallized within the layer as a result.[23] The formation of lithium compounds such as $LiYO_2$ and $Li_2Si_2O_5$ were not detected by XRD.

The densification, mechanical and thermal properties of Si_3N_4 sintered with Y_2O_3 (and SiO_2) have been intensively

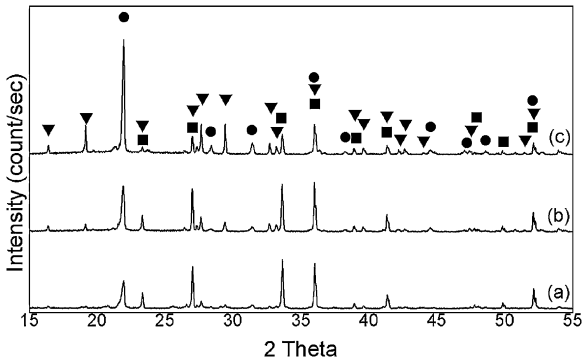

Fig. 5. XRD data of the sample surface after the bending test at 1300 °C in air. (a) 7.5-1650, (b) 10-1650 and (c) 12.5-1650 specimen (■: Si_3N_4, ●: SiO_2, ▼: $Si_2Y_2O_7$).

investigated. In many cases the products were densified above 1825 °C and/or under high pressure.[17,18,24–26] The room temperature strength of Y_2O_3–Si_3N_4 systems was reported to be 332–662 MPa.[18,24] The Y_2O_3–Si_3N_4 system has excellent high temperature strength (628 MPa at 1350 °C, 434 MPa at 1370 °C and 472 MPa at 1400 °C).[18,24,25] Although the high temperature strength of the $LiYO_2$–Si_3N_4 system was not as good as that of the Y_2O_3–Si_3N_4 system in spite of the strong reduction of Li content (431 MPa at 1300 °C), the system clearly has benefits compared to the system without Li in terms of densification and strength at ambient condition, both of which are important factors for the commercialization of Si_3N_4.

4. Conclusions

The residual Li content of a pressureless sintered $LiYO_2$–Si_3N_4 system was decreased down to 0.008 wt% after the annealing at 1650 °C for 8 h. The most appropriate additive content among the tested conditions for the removal of Li was 7.5 wt%. The oxidation resistance, high temperature strength and creep resistance of the $LiYO_2$–Si_3N_4 system were clearly improved by vaporizing residual Li. Different from the former methods, such as using rare-earth oxide additives or the crystallization of amorphous grain boundary phase, the high temperature properties of Si_3N_4 could be improved without requiring excessively high temperature, high pressure or prolonged annealing time and without sacrificing the mechanical properties by removing a vaporizing additive through an annealing treatment.

Acknowledgement

The kind and intensive discussion of Prof. F. Aldinger and Dr. G. Rixecker is greatly appreciated.

References

1. Riley, F., Silicon nitride and related materials. *J. Am. Ceram. Soc.*, 2000, **83**(2), 245–265.
2. Zhu, X. W., Suzuki, T. S., Uchikoshi, T., Nishimura, T. and Sakka, Y., Texture development in Si_3N_4 ceramics by magnetic field alignment during slip casting. *J. Ceram. Soc. Jpn.*, 2006, **114**(1335), 979–987.
3. Wasanapiarnpong, T., Wada, S., Imai, M. and Yano, T., Lower temperature pressureless sintering of Si_3N_4 ceramics using SiO_2–MgO–Y_2O_3 additives without packing powder. *J. Ceram. Soc. Jpn.*, 2006, **114**(1333), 733–738.
4. Matovic, B., Rixecker, G. and Aldinger, F., Densification of Si_3N_4 with $LiYO_2$ additives. *J. Am. Ceram. Soc.*, 2004, **87**(4), 546–549.
5. Matovic, B., Rixecker, G. and Aldinger, F., Pressureless sintering of silicon nitride with Lithia and yttria. *J. Eur. Ceram. Soc.*, 2004, **24**(12), 3395–3398.
6. Lee, S. H., Low-temperature pressureless sintering of $LiYO_2$–Si_3N_4 and effect of annealing on the microstructure and room temperature properties. *Int. J. Appl. Ceram. Technol.*, in press.
7. Guo, S., Hirosaki, N., Yamamoto, Y., Nishimura, T. and Mitomo, M., Strength retention in hot-pressed Si_3N_4 ceramics with Lu_2O_3 additives after oxidation exposure in air at 1500 °C. *J. Am. Ceram. Soc.*, 2002, **85**(6), 1607–1609.
8. Subramaniam, A., Koch, C. T., Cannon, R. M. and Ruehle, M., Intergranular glassy films: an overview. *Mater. Sci. Eng. A*, 2006, **422**, 3–8.
9. Zou, Y. and Petric, A., Thermodynamic stability of lithium zirconates and lithium yttrate. *J. Phys. Chem. Solid*, 1994, **55**(6), 494–499.
10. *Standard Test Method for Flexural Strength of Advanced Ceramics at Ambient Temperature*. ASTM, 1991, pp. C1161–1190.
11. Anstis, G. R., Chantikul, P., Lawn, B. R. and Marshall, D. B., A critical evaluation of indentation techniques for measuring fracture toughness. 1. Direct crack measurements. *J. Am. Ceram. Soc.*, 1981, **64**(9), 534–538.
12. Watari, K., Hwang, H. J., Toriyama, M. and Kanzaki, S., Effective sintering aids for low-temperature sintering of AlN ceramics. *J. Mater. Res.*, 1999, **14**(4), 1409–1417.
13. Ordoñez, S., Iturriza, I. and Castro, F., The influence of amount and type of additives on $\alpha \rightarrow \beta$ Si_3N_4 transformation. *J. Mater. Sci.*, 1999, **34**(1), 147–153.
14. Hwang, C. J., Susnitzky, D. W., Newman, R. A., Beaman, D. R. and Pyzik, A. J., Controlled crystallization in self-reinforced silicon nitride with Y_2O_3, SrO and CaO: crystallization behaviour. *J. Am. Ceram. Soc.*, 1995, **78**(11), 3072–3080.
15. Ge, C. C., Liu, W. S., Xia, Y. L. and Chen, L. M., Oxidation behavior of Si_3N_4–ZrN–AlN ceramics. In *Key Engineering Materials*, *Vols. 89–91*, ed. M. J. Hoffmann, P. F. Becher and G. Petzow. Trans Tech Publication, Zuelich, Switzerland, 1994, pp. 307–311.
16. Oliveira, F. A. C., Baxter, D. J. and Ungeheuer, J., Modeling of the oxidation kinetics of a yttria-doped hot-pressed silicon nitride. *J. Eur. Ceram. Soc.*, 1998, **18**(16), 2307–2317.
17. Chen, J., Sjoeberg, J., Lindqvist, O., O'Meara, C. and Pejryd, L., The rate-controlling processes in the oxidation of HIPed Si_3N_4 with and without sintering additives. *J. Eur. Ceram. Soc.*, 1991, **7**(2), 319–327.
18. Govila, R. K., Mangels, J. A. and Bear, J. R., Fracture of yttria-doped, sintered reaction-bonded silicon nitride. *J. Am. Ceram. Soc.*, 1985, **68**(7), 413–418.
19. Levin, E. M. and Mcmurdie, H. F. ed., *Phase Diagram for Ceramists*, *vol. 2*. The American Ceramic Society, Columbus, OH, 1975, Fig. 2388.
20. Wiederhorn, S. M. and Tighe, N. J., Structural reliability of yttria-doped hot-pressed silicon nitride at elevated temperatures. *J. Am. Ceram. Soc.*, 1983, **66**(12), 884–889.
21. Mieskowski, D. M. and Sanders, W. A., Oxidation of silicon nitride sintered with rare-earth oxide additions. *J. Am. Ceram. Soc.*, 1985, **68**(7), C160–C163.
22. Jacobson, N. S., Corrosion of silicon-based ceramics in combustion environments. *J. Am. Ceram. Soc.*, 1993, **76**, 3–28.
23. Ukyo, Y., The effect of a small amount of impurity on the oxidation of Si_3N_4 ceramics. *J. Mater. Sci.*, 1997, **32**(20), 5483–5489.
24. Clarke, D. R., Lange, F. F. and Schnittgrund, G. D., Strengthening of a sintered silicon nitride by a post-fabrication heat treatment. *Commun. Am. Ceram. Soc.*, 1982, **65**, C51–C52.
25. Rho, H., Hecht, N. L. and Graves, G. A., Effect of water vapor on the mechanical behaviors of hot isostatically pressed silicon nitride containing Y_2O_3. *J. Mater. Sci.*, 2000, **35**, 3415–3423.
26. Babini, G. N., Bellosi, A. and Vincenzini, P., Factors influencing structural evolution in the oxide of hot-pressed Si_3N_4–Y_2O_3–SiO_2 materials. *J. Mater. Sci.*, 1984, **19**, 3487–3497.